

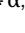




Supplementary Material for:
A record of magmatic differentiation in plutonic xenoliths from Santorini
(Greece)

Sean Whitley^α,  Ralf Halama*^{α,β},  Ralf Gertisser^α,  Thor H. Hansteen^γ,  Matthias Frische^γ, and
 Torsten Vennemann^δ

^α School of Geography, Geology and the Environment, Keele University, Keele, ST5 5BG, UK.

^β Institute of Geosciences and Geography, Martin-Luther-Universität Halle-Wittenberg, Von-Seckendorff-Platz 3, 06120 Halle (Saale), Germany.

^γ GEOMAR Helmholtz Centre for Ocean Research Kiel, Wischhofstrasse 1-3, D-24148 Kiel, Germany.

^δ Faculty of Geosciences and Environment, Université de Lausanne, CH-1015 Lausanne, Switzerland.

This supplementary material accompanies the article:

Whitley, S., Halama, R., Gertisser, R., Hansteen, T. H., Frische, M., and Vennemann, T. (2024) "A record of magmatic differentiation in plutonic xenoliths from Santorini (Greece)", *Volcanica*, 7(2), pp. 421–446. DOI: <https://doi.org/10.30909/vol.07.02.421446>.

Whitley et al. (2024) should be cited if this material is used independently of the article.

A1 ANALYTICAL METHODS

A1.1 Electron microprobe

Major element concentrations in minerals, and major element, chlorine and sulphur concentrations in interstitial glasses and melt inclusions were determined with a JXA 8900 electron microprobe at the University of Kiel, Germany. Silicate and oxide minerals were analysed with a 2 μm beam diameter, 15 kV accelerating voltage and 15 nA beam current. Glasses were measured with a 5 μm defocused beam at 15 kV accelerating voltage and a 12 nA beam current. Na was measured first to minimise Na-loss. Measurement times were 15 s peak and 7 s background, excluding S, Cl, and P, which were measured for 60 s peak and 30 s background. Natural mineral standards (topaz, rutile, baryte, tugtupite, fayalite, forsterite, mica, anorthite, wollastonite, apatite, tephroite) were used for calibration and Smithsonian basaltic glass A-99, forsterite 83 (USNM 2566), plagioclase (USNM 115900), garnet RV2 (USNM 87375), and obsidian ASTIMEX Block SPGLASS7 were used as secondary within-run standards to assess accuracy and precision (see Table S1 in [Supplementary Material 2](#)). Relative accuracy and precision are better than 5 % for major elements and 10 % for minor elements. A CITZAF matrix correction was applied. All Mg# values were calculated assuming all Fe as Fe²⁺ using $Mg\# = Mg/(Mg + Fe_{total})$. Fe³⁺ was estimated for clinopyroxene from stoichiometry using formulations by [Droop \[1987\]](#).

A1.2 Laser Ablation - Inductively Coupled Plasma - Mass Spectrometry (LA-ICP-MS)

Trace elements in minerals and glasses were analysed at the GEOMAR Helmholtz Centre for Ocean Research Kiel using a

Nu Instruments AttoM HR-ICP-MS connected to a Coherent GeoLasPro 193 nm Excimer laser ablation system. Spot analyses on samples were done by 30 s ablation at a laser repetition rate of 10 Hz and a fluence of 5 J/cm² using 44 μm spot diameter for silicate minerals and 24 μm for glasses. 50 s gas background were collected prior to each ablation. Measurements were made on the same polished sections used for EMPA to provide a robust internal standard using the sum of ²⁹Si and ⁴³Ca for internal standardization. The NIST 610 standard reference material (SRM) was used for mass calibration. Repeated measurements of the USGS basaltic glasses BCR-2G and BHVO-2G as secondary SRMs were made throughout each analytical session to check accuracy and precision (see Table S2 in [Supplementary Material 2](#)). Measurements were made in blocks of 8 samples and 8 SRMs to minimise the effects of instrumental drift. Data evaluation has been performed applying the linear regression slope method [[Fietzke et al. 2008](#)]. Full details of the analytical setup are provided in [Fietzke and Frische \[2016\]](#).

A1.3 Whole-rock geochemistry

Samples were powdered at Keele University after washing and removal of surface altered material, using a jaw crusher followed by an agate mill. Whole-rock analyses were carried out for 8 samples by Bureau Veritas (AcmeLabs), Canada, by X-ray fluorescence (XRF). Samples were fused with a lithium tetraborate flux in a crucible before analysis of major and selected trace elements. For oxides >1 wt%, two internal standards reproduced expected values to better than 3 %. Due to sample size constraints, whole-rock compositions for an additional 7 samples were determined by point counting (1000–2000 points; [[Whitley et al. 2020](#)]). Averaged mineral and glass compositions were used with the phase volumes counted, corrected for varying mineral and glass densities using mineral

*✉ ralf.halama@geo.uni-halle.de

densities from [Deer et al. \[1997\]](#). The bulk compositions were obtained using the Rock-Maker spreadsheet [[Büttner 2012](#)], which generates bulk whole rock compositions from phase volumes and densities.

A1.4 Mineral Oxygen Isotope Analysis

Minerals were picked from sieved grain size fractions (125 and 63 microns) of powdered rocks at Keele University, using magnetic separation to remove minerals with magnetite inclusions. Minerals were then washed in diluted HCl. Oxygen isotope analyses were carried out in the Stable Isotope Laboratory of the University of Lausanne using a CO₂-laser fluorination line linked to a Finnigan MAT 253 gas-source mass spectrometer. The methodology is based on [Sharp \[1990\]](#) and described in detail in [Lacroix and Vennemann \[2015\]](#). Between 1.4 and 2.4 mg of sample material was used for the analyses. Oxygen isotope compositions are presented in the standard δ -notation relative to Vienna Standard Mean Ocean Water (VSMOW) in per mil (‰). The in-house quartz standard LS-1 with an accepted value of 18.1 ‰ [[Seitz et al. 2016](#)] was measured to evaluate analytical uncertainty. During the course of this study, measurements of LS-1 quartz gave 18.10 ± 0.11 ‰ (1 standard deviation, $n = 5$).

A2 MELT INCLUSION POST-ENTRAPMENT CRYSTALLISATION (PEC)

Melt inclusion compositions can be modified by post entrapment processes such as diffusive equilibration and crystallisation on the melt-crystal interface [e.g. [Danyushevsky et al. 2000](#); [Kent 2008](#); [Nielsen 2011](#)]. Therefore, care is required in establishing whether the melt inclusions represent typical melt compositions of the host magmatic system. As is common in plutonic material, many samples contain melt inclusions that show clear textural evidence for post-entrapment modification, such as dusting (devitrification) and crystallisation within the inclusion, which varies with host phase and sample. Only melt inclusions with a clear glassy appearance were selected for analysis. Melt inclusion major element data have been corrected for post entrapment crystallisation using methodologies summarised for individual minerals below and described in detail in [Whitley et al. \[2020\]](#). The compositions of melt inclusions are assessed relative to the liquid line of descent and corrections are applied to melt inclusions that appear to have been modified. These corrections assume the trapped melt was originally in equilibrium with the host mineral, and plot within the liquid line of descent for Santorini magmas.

A2.1 Olivine-hosted inclusions

Olivine-hosted melt inclusions fall outside the liquid line of descent and show a strong elevation in CaO/Al₂O₃ and depletion in Fe (Fe loss: [Danyushevsky et al., 2000](#)), coupled with $K_{D_{Fe-Mg}^{olivine-melt}}$ values below the equilibrium range of 0.3 ± 0.03 [[Toplis 2005](#); [Putirka 2008](#)]. These melt inclusions were corrected for post entrapment modification using PetroLog [[Danyushevsky and Plechov 2011](#)]. The original melt FeO* is estimated based on the amount of FeO* required to bring

the inclusions back to the liquid line of descent, and comparison with clinopyroxene and plagioclase hosted melt inclusion compositions. [Ford et al. \[1983\]](#) was used as the olivine-melt model and fugacity was set at QFM [[Gertisser et al. 2009](#)]. PEC corrections required 0.5 to 17.9 % olivine addition.

A2.2 Clinopyroxene- and orthopyroxene-hosted inclusions

We follow the methodology of [Bali et al. \[2018\]](#) by adding host clinopyroxene to the melt inclusion until $K_{D_{Fe-Mg}^{cpx-melt}} = 0.28$ is reached. This approach requires plausible correction percentages (<20 %) and yields Al₂O₃ concentrations that overlap the literature volcanic rock data and interstitial glasses analysed in this study ([Whitley, 2020](#)). Melt inclusions in orthopyroxene were corrected by adding the host orthopyroxene back to the inclusion until $K_{D_{Fe-Mg}^{opx-melt}} = 0.29 \pm 0.06$ [[Putirka 2008](#)] is approached, which produced plausible melt compositions that follow the liquid line of descent and overlapping interstitial glass analyses, requiring less than 8 % orthopyroxene addition.

A2.3 Plagioclase-hosted inclusions

PEC of plagioclase-hosted melt inclusions is evidenced by a fine micron-scale rim of lower An plagioclase around melt inclusion rims, and elements strongly compatible in plagioclase such as Al₂O₃ diverging from the liquid line of descent along a plagioclase crystallisation vector [[Whitley et al. 2020](#)]. These inclusions were corrected following the approach of [Neave and Putirka \[2017\]](#) and [Bali et al. \[2018\]](#), where the original melt inclusion composition is assumed to lie on the liquid line of descent. Host plagioclase composition is added back to the inclusion until the Al₂O₃ vs MgO concentration in the melt inclusion approximates that predicted by a linear regression through the literature volcanic whole rock and glass dataset. This results in 9 to 19 % plagioclase addition.

A3 THERMOBAROMETRY

Several mineral-only and mineral-melt thermobarometers were applied to the xenoliths to place constraints on the temperature and pressure of xenolith formation. As the interstitial liquids found within the xenoliths are often too felsic to be in equilibrium with the coexisting minerals, and some xenoliths may not be cogenetic with the eruptive layers they are found in, several mineral-melt equilibria models were used to determine a range of plausible equilibrium liquids from known Santorini liquid compositions. An extensive database of Santorini whole rock, melt inclusion and groundmass glass analyses from the literature ($n=1226$) and this study ($n=118$) were paired with each mineral phase and plausible pairs were filtered via equilibrium tests [[Putirka 1999](#); [Putirka 2008](#); [Mollo et al. 2013](#); [Neave et al. 2013](#); [Neave and Putirka 2017](#)]. A detailed assessment of the equilibrium tests, effects of iterative calculations and applicability of the thermobarometers to Santorini compositions is given in [Whitley et al. \[2020\]](#) and key aspects are summarised in the following.

Clinopyroxene, orthopyroxene and plagioclase were paired with plausible liquids using this method and thermobarometers were solved iteratively; barometers were paired to ther-

mometers. As most thermobarometric equations are H₂O sensitive but most potential liquids in the database used for mineral melt thermobarometry lack water measurements, published water content measurements were used to develop a linear model to estimate water contents in the melt as a function of SiO₂ (Whitley, 2020). A new plagioclase liquid equilibrium test is derived from a large experimental dataset including Santorini experiments [Blundy and Wood 1994; Cadoux et al. 2014; Andújar et al. 2015; 2016] based on X_{liquid}^{Si} and is used instead of the two-temperature bracketed test of Putirka [2008]:

$$\ln(KD_{Plagioclase-Liquid}^{Ab-An}) \pm 0.4541 = 1.26954 - 5.38702X_{liquid}^{Si}. \quad (1)$$

Olivine-melt thermometry was based on using both equations 21 and 22 of Putirka [2008] on post-entrapment crystallisation-corrected (PETROLOG [Danyushevsky and Plechov 2011]) melt inclusion compositions and paired with equilibrium melts. For clinopyroxene, the most accurate thermometer and barometer combination is using equation 33 of Putirka [2008] (temperature) paired with equation 32b (pressure). Orthopyroxene thermobarometers (equations 28, 29a, 29b in Putirka [2008]) perform well for experiments with relevant compositions, but overestimate pressures in the < 5 kbar pressure range applicable to Santorini, so that a 2 kbar pressure correction is applied to these results. For plagioclase-melt equilibria, the results from plagioclase thermometry and hygrometry are paired with a constant value of 2 kbar, which is the average of results of barometry from clinopyroxene and orthopyroxene-melt calculations.

A4 TRACE ELEMENT PARTITION COEFFICIENTS

Partition coefficients for mineral-melt exchange were calculated for three minerals based on the sources indicated: plagioclase [Bédard 2006], clinopyroxene [Bédard 2014], and orthopyroxene [Bédard 2007]. These models use regressions through extensive experimental databases and observed natural partitioning values to calculate partition coefficients based on mineral and/or melt variables. These were chosen over the lattice strain model [Blundy and Wood 1994] and recent models built upon this [e.g. Hill et al. 2011; Sun and Liang 2012; Sun et al. 2017] as the Bédard models are calibrated over a wider range of mineral compositions, melt compositions and temperature, applicable for the large variations seen within the xenoliths. For clinopyroxene rare earth element partition coefficients, nearest neighbour parameterisations were used based on an initial calculation of LnD Sm, as recommended by Bédard [2014]. Each neighbour element is predicted with an R² > 0.95 from this initial partition coefficient. Calculated plagioclase partition coefficients take the form $RT \ln D$, therefore temperature is estimated using plagioclase molar An content [Druitt et al. 2012; Fabbro et al. 2018], consistent with our temperatures calculated from plagioclase-melt thermobarometry using the equation from [Druitt et al. 2012]:

$$T(K) = 1128 + 200 \frac{X_{An} - 0.4}{0.4}. \quad (2)$$



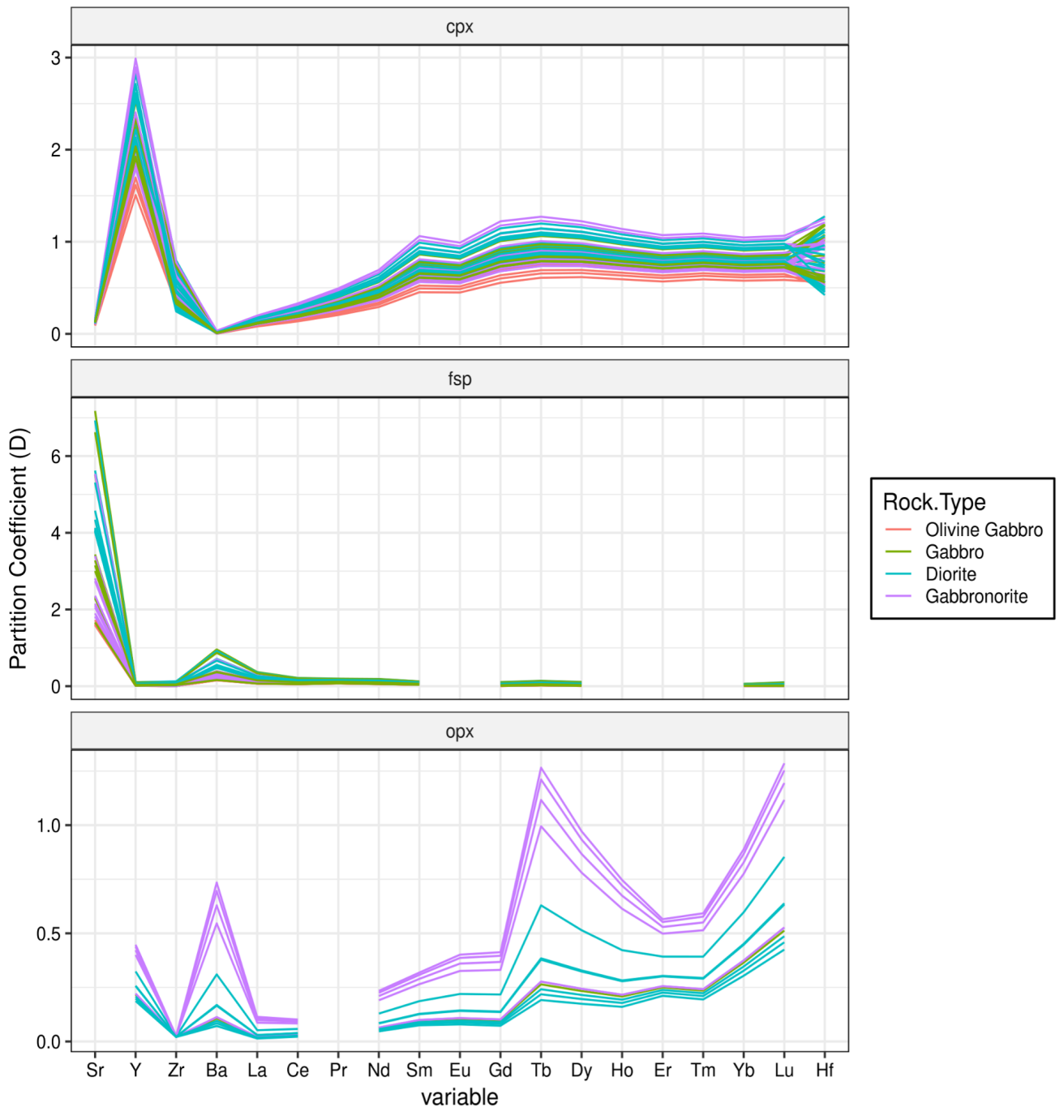


Figure S1: Partition coefficients for clinopyroxene (cpx), feldspar (fsp) and orthopyroxene (opx) used in this study. Partition coefficients were calculated using the models described the text.

COPYRIGHT

© The Author(s) 2024. This article is distributed under the terms of the [Creative Commons Attribution 4.0 International License](https://creativecommons.org/licenses/by/4.0/), which permits unrestricted use, distribution, and reproduction in any medium, provided you give appropriate credit to the original author(s) and the source, provide a link to the Creative Commons license, and indicate if changes were made.

REFERENCES

- Andújar, J., B. Scaillet, M. Pichavant, and T. Druitt (2015). “Differentiation conditions of a basaltic magma from Santorini, and its bearing on the production of andesite in arc settings”. In: *Journal of Petrology* 56, pages 765–794. DOI: [10.1093/petrology/egv016](https://doi.org/10.1093/petrology/egv016).
- (2016). “Generation Conditions of Dacite and Rhyodacite via the Crystallization of an Andesitic Magma. Implications for the Plumbing System at Santorini (Greece) and the Origin of Tholeiitic or Calc-alkaline Differentiation Trends in Arc Magmas”. In: *Journal of Petrology* 57, pages 1887–1920. DOI: [10.1093/petrology/egw061](https://doi.org/10.1093/petrology/egw061).
- Bali, E., M. E. Hartley, S. A. Halldórsson, G. H. Gudfinnsson, and S. Jakobsson (2018). “Melt inclusion constraints on volatile systematics and degassing history of the 2014–2015 Holuhraun eruption, Iceland”. In: *Contributions to Mineralogy and Petrology* 173(2). DOI: [10.1007/s00410-017-1434-1](https://doi.org/10.1007/s00410-017-1434-1).
- Bédard, J. H. (2006). “Trace element partitioning in plagioclase feldspar”. In: *Geochimica et Cosmochimica Acta* 70, pages 3717–3742. DOI: [10.1016/j.gca.2006.05.003](https://doi.org/10.1016/j.gca.2006.05.003).
- (2007). “Trace element partitioning coefficients between silicate melts and orthopyroxene: parameterizations of D variations”. In: *Chemical Geology* 244, pages 263–303. DOI: [10.1016/j.chemgeo.2007.06.019](https://doi.org/10.1016/j.chemgeo.2007.06.019).
- (2014). “Parameterizations of calcic clinopyroxene–Melt trace element partition coefficients”. In: *Geochemistry, Geophysics, Geosystems* 15, pages 303–336. DOI: [10.1002/2013GC005112](https://doi.org/10.1002/2013GC005112).
- Blundy, J. and B. Wood (1994). “Prediction of crystal–melt partition coefficients from elastic moduli”. In: *Nature* 372, pages 452–454. DOI: [10.1038/372452a0](https://doi.org/10.1038/372452a0).
- Büttner, S. H. (2012). “Rock Maker: an MS Excel™ spreadsheet for the calculation of rock compositions from proportional whole rock analyses, mineral compositions, and modal abundance”. In: *Mineralogy and Petrology* 104(1–2), pages 129–135. DOI: [10.1007/s00710-011-0181-7](https://doi.org/10.1007/s00710-011-0181-7).
- Cadoux, A., B. Scaillet, T. Druitt, and E. Deloule (2014). “Magma storage conditions of large Plinian eruptions of Santorini Volcano (Greece)”. In: *Journal of Petrology* 55, pages 1129–1171. DOI: [10.1093/petrology/egu021](https://doi.org/10.1093/petrology/egu021).
- Danyushevsky, L. V., F. N. Della-Pasqua, and S. Sokolov (2000). “Re-equilibration of melt inclusions trapped by magnesian olivine phenocrysts from subduction-related magmas: petrological implications”. In: *Contributions to Mineralogy and Petrology* 138(1), pages 68–83. DOI: [10.1007/pl00007664](https://doi.org/10.1007/pl00007664).
- Danyushevsky, L. V. and P. Plechov (2011). “Petrolog3: Integrated software for modeling crystallization processes: PÉTROLOG3”. In: *Geochemistry, Geophysics, Geosystems* 12(7). DOI: [10.1029/2011gc003516](https://doi.org/10.1029/2011gc003516).
- Deer, W. A., R. A. Howie, and J. Zussman (1997). *Rock-Forming Minerals*. 2nd edition. Geological Society of London.
- Droop, G. T. R. (1987). “A general equation for estimating Fe³⁺ concentrations in ferromagnesian silicates and oxides from microprobe analyses, using stoichiometric criteria”. In: *Mineralogical Magazine* 51(361), pages 431–435. DOI: [10.1180/minmag.1987.051.361.10](https://doi.org/10.1180/minmag.1987.051.361.10).
- Druitt, T., F. Costa, E. Deloule, M. Dungan, and B. Scaillet (2012). “Decadal to monthly timescales of magma transfer and reservoir growth at a caldera volcano”. In: *Nature* 482, pages 77–80. DOI: [10.1038/nature10706](https://doi.org/10.1038/nature10706).
- Fabbro, G., T. Druitt, and F. Costa (2018). “Storage and eruption of silicic magma across the transition from dominantly effusive to caldera-forming states at an arc volcano (Santorini, Greece)”. In: *Journal of Petrology* 58, pages 2429–2464. DOI: [10.1093/petrology/egy013](https://doi.org/10.1093/petrology/egy013).
- Fietzke, J. and M. Frische (2016). “Experimental evaluation of elemental behavior during LA-ICP-MS: influences of plasma conditions and limits of plasma robustness”. In: *Journal of Analytical Atomic Spectrometry* 31(1), pages 234–244. DOI: [10.1039/c5ja00253b](https://doi.org/10.1039/c5ja00253b).
- Fietzke, J., V. Liebetrau, D. Günther, K. Gürs, K. Hametner, K. Zumholz, T. H. Hansteen, and A. Eisenhauer (2008). “An alternative data acquisition and evaluation strategy for improved isotope ratio precision using LA-MC-ICP-MS applied to stable and radiogenic strontium isotopes in carbonates”. In: *Journal of Analytical Atomic Spectrometry* 23(7), page 955. DOI: [10.1039/b717706b](https://doi.org/10.1039/b717706b).
- Ford, C. E., D. G. Russell, J. A. Craven, and M. R. Fisk (1983). “Olivine-Liquid Equilibria: Temperature, Pressure and Composition Dependence of the Crystal/Liquid Cation Partition Coefficients for Mg, Fe²⁺, Ca and Mn”. In: *Journal of Petrology* 24(3), pages 256–266. DOI: [10.1093/petrology/24.3.256](https://doi.org/10.1093/petrology/24.3.256).
- Gertisser, R., K. Preece, and J. Keller (2009). “The Plinian Lower Pumice 2 eruption, Santorini, Greece: magma evolution and volatile behaviour”. In: *Journal of Volcanology and Geothermal Research* 186, pages 387–406. DOI: [10.1016/j.jvolgeores.2009.07.015](https://doi.org/10.1016/j.jvolgeores.2009.07.015).
- Hill, E., J. D. Blundy, and B. J. Wood (2011). “Clinopyroxene–melt trace element partitioning and the development of a predictive model for HFSE and Sc”. In: *Contributions to Mineralogy and Petrology* 161(3), pages 423–438. DOI: [10.1007/s00410-010-0540-0](https://doi.org/10.1007/s00410-010-0540-0).
- Kent, A. J. (2008). “Melt Inclusions in Basaltic and Related Volcanic Rocks”. In: *Reviews in Mineralogy and Geochemistry* 69(1), pages 273–331. DOI: [10.2138/rmg.2008.69.8](https://doi.org/10.2138/rmg.2008.69.8).
- Lacroix, B. and T. Vennemann (2015). “Empirical calibration of the oxygen isotope fractionation between quartz and Fe–Mg-chlorite”. In: *Geochimica et Cosmochimica Acta* 149, pages 21–31. DOI: [10.1016/j.gca.2014.10.031](https://doi.org/10.1016/j.gca.2014.10.031).

- Mollo, S., K. Putirka, V. Misiti, M. Soligo, and P. Scarlato (2013). “A new test for equilibrium based on clinopyroxene–melt pairs: Clues on the solidification temperatures of Etnean alkaline melts at post-eruptive conditions”. In: *Chemical Geology* 352, pages 92–100. DOI: [10.1016/j.chemgeo.2013.05.026](https://doi.org/10.1016/j.chemgeo.2013.05.026).
- Neave, D. and K. Putirka (2017). “A new clinopyroxene-liquid barometer, and implications for magma storage pressures under Icelandic rift zones”. In: *American Mineralogist* 102, pages 777–794. DOI: [10.2138/am-2017-5968](https://doi.org/10.2138/am-2017-5968).
- Neave, D. A., E. Passmore, J. Maclennan, G. Fitton, and T. Thordarson (2013). “Crystal–Melt Relationships and the Record of Deep Mixing and Crystallization in the ad 1783 Laki Eruption, Iceland”. In: *Journal of Petrology* 54(8), pages 1661–1690. DOI: [10.1093/petrology/egt027](https://doi.org/10.1093/petrology/egt027).
- Nielsen, R. L. (2011). “The effects of re-homogenization on plagioclase hosted melt inclusions: TECHNICAL BRIEF”. In: *Geochemistry, Geophysics, Geosystems* 12(10). DOI: [10.1029/2011gc003822](https://doi.org/10.1029/2011gc003822).
- Putirka, K. (2008). “Thermometers and barometers for volcanic systems”. In: *Reviews in Mineralogy and Geochemistry* 69, pages 61–120. DOI: [10.2138/rmg.2008.69.3](https://doi.org/10.2138/rmg.2008.69.3).
- Putirka, K. (1999). “Clinopyroxene + liquid equilibria to 100 kbar and 2450 K”. In: *Contributions to Mineralogy and Petrology* 135(2–3), pages 151–163. DOI: [10.1007/s004100050503](https://doi.org/10.1007/s004100050503).
- Seitz, S., L. P. Baumgartner, A.-S. Bouvier, B. Putlitz, and T. Vennemann (2016). “Quartz Reference Materials for Oxygen Isotope Analysis by <sc>SIMS</sc>”. In: *Geostandards and Geoanalytical Research* 41(1), pages 69–75. DOI: [10.1111/ggr.12133](https://doi.org/10.1111/ggr.12133).
- Sharp, Z. D. (1990). “A laser-based microanalytical method for the in situ determination of oxygen isotope ratios of silicates and oxides”. In: *Geochimica et Cosmochimica Acta* 54(5), pages 1353–1357. DOI: [10.1016/0016-7037\(90\)90160-m](https://doi.org/10.1016/0016-7037(90)90160-m).
- Sun, C., M. Graff, and Y. Liang (2017). “Trace element partitioning between plagioclase and silicate melt: The importance of temperature and plagioclase composition, with implications for terrestrial and lunar magmatism”. In: *Geochimica et Cosmochimica Acta* 206, pages 273–295. DOI: [10.1016/j.gca.2017.03.003](https://doi.org/10.1016/j.gca.2017.03.003).
- Sun, C. and Y. Liang (2012). “Distribution of REE between clinopyroxene and basaltic melt along a mantle adiabat: effects of major element composition, water, and temperature”. In: *Contributions to Mineralogy and Petrology* 163, pages 807–823. DOI: [10.1007/s00410-011-0700-x](https://doi.org/10.1007/s00410-011-0700-x).
- Toplis, M. J. (2005). “The thermodynamics of iron and magnesium partitioning between olivine and liquid: criteria for assessing and predicting equilibrium in natural and experimental systems”. In: *Contributions to Mineralogy and Petrology* 149(1), pages 22–39. DOI: [10.1007/s00410-004-0629-4](https://doi.org/10.1007/s00410-004-0629-4).
- Whitley, S., R. Halama, R. Gertisser, K. Preece, F. Deegan, and V. Troll (2020). “Magmatic and Metasomatic Effects of Magma–Carbonate Interaction Recorded in Calc-silicate Xenoliths from Merapi Volcano (Indonesia)”. In: *Journal of Petrology* 61, ega048. DOI: [10.1093/petrology/egaa048](https://doi.org/10.1093/petrology/egaa048).